CHEMICAL ENGINEERING TRANSACTIONS
VOL. 70, 2018
A publication of AIDIC
The Italian Association of Chemical Engineering
Online at www.aidic.it/cet
Guest Editors: Timothy G. Walmsley, Petar S. Varbanov, Rongxin Su, Jiří J. Klemeš

ISBN 978-88-95608-67-9; **ISSN** 2283-9216
DOI: 10.3303/CET1870294

Mathematical Modelling of the Process of Spark Plasma Sintering of a Ceramic Material Composite Al_2O_3 - ZrO_2 - Y_2O_3, Modified by Carbon Nanotubes

Natasha V. Mamonova*, Eleonora Koltsova, Evgenia A. Skichko, Anna S. Shaneva, Nelly A. Popova

D. Mendeleyev University of Chemical Technology of Russia, Miusskaya sq. 9, 125047 Moscow, Russia
kolts@muctr.ru

Experimental studies have been carried out in the field of obtaining carbon nanotubes (CNT) and Al_2O_3 - ZrO_2 - Y_2O_3 composite reinforced with CNTs. Mathematical models of CNT synthesis and spark plasma sintering of a composite have been developed. On the basis of experimental studies and mathematical modeling, optimal conditions for CNT synthesis and sintering of the Al_2O_3 - ZrO_2 - Y_2O_3 - CNT composite have been determined.

1. Introduction

The rapid pace of technological development, and the modernization of technology, present new, higher requirements for existing materials. Therefore, in the modern world a large and growing demand for new construction materials arose.
Creation of composites based on corundum-zirconium ceramics is one of the intensively developed areas of modern materials science, in view of the unique combination of properties that such materials can possess, while the use of nanotubes as a modifying additive allows to significantly improve the mechanical, heat and electrically conductive properties of ceramics, and also reduce the sintering temperature.
Sparkling plasma sintering (SPS) is a sintering technique that uses uniaxial force and pulsating directional electric current at low atmospheric pressure to obtain a high rate of consolidation of the powder. This makes it possible to apply high heating and cooling rates that increase the compaction by contributing to the diffusion mechanisms of grain growth and preserving the intrinsic properties of the powder nanoparticles in the final dense article.
SPS is a fast sintering method in which heating is not homogeneously distributed throughout the volume of the powder compact on a macroscopic scale, but in addition, thermal energy is distributed precisely in those places on a microscopic scale, where energy is required for the sintering process, namely at points contact of the particles of the sintered powder. This fact leads to the fact that sintering is accompanied by a smaller grain growth (Suárez et al., 2013). The mechanical properties of composites are improved due to the modification of CNTs (Fedosova et al., 2015).
The purpose of this work is both research in the field of CNT synthesis and research in the field of nanocomposite production reinforced with CNTs for the subsequent optimization of sintering parameters and the production of composites with zero porosity and high strength characteristics.

2. Experimental research

2.1 Experimental research in the field of CNT synthesis by catalytic pyrolysis of a methane-hydrogen mixture

Table 1 shows the composition of the catalyst components for the production of carbon nanotubes (CNTs) by catalytic pyrolysis of a methane-hydrogen mixture. The investigations were carried out according to the procedure presented by Skichko et al. (2012) and Bogdanovskaya et al. (2016).

Please cite this article as: Mamonova N.V., Koltsova E.M., Skichko E.A., Shaneva A.S., Popova N.A., 2018, Mathematical modelling of the process of spark plasma sintering of a ceramic material composite al2o3 - zro2 - y2o3, modified by carbon nanotubes , Chemical Engineering Transactions, 70, 1759-1764 DOI:10.3303/CET1870294

Table 1: Specific yields of carbon nanotubes on catalysts with different composition of active phase

№	Composition of catalyst	Output of CNT, g/gKt	External diameter of CNT, nm	Inner diameter of CNT, nm	Number of layers	Bulk density of CNT, g/cm^3
1	$[Fe_{0,60}Al_{0,40}]_2O_3$	22.4	10-20	2-10	15-20	0.040
2	$[Fe_{0,45}Co_{0,15}Al_{0.40}]_2O_3$	31	5-15	2-10	10-17	0.038
3	$[Fe_{0,30}Co_{0,30}Al_{0,40}]_2O_3$	30.3	10-20	2-15	6-10	0.031
4	$[Fe_{0,15}Co_{0,45}Al_{0,40}]_2O_3$	30	10-30	5-20	8-25	0.029
5	$[Co_{0,60}Al_{0,40}]_2O_3$	28.13	10-35	5-15	15-30	0.027

Table 1 shows that the yields of carbon nanotubes were in the range 22.4-31 g / g KT. The highest yield was obtained on the catalyst $(Fe_{0.45}Co_{0.15}Al_{0.40})_2O_3$ and amounted to 31 g/gKt. The obtained CNTs have 10-17 layers with internal partitions. The outer diameter is 5-15 nm, the internal diameter is 2-10 nm.The second series of experiments was related to the study of the influence of temperature on the synthesis of CNTs. An investigation of the effect of temperature on the kinetics of the synthesis of carbon nanotubes was carried out in the temperature range 700-800 ° C (step at 25 ° C), the catalyst charge was 5 mg.

The kinetic curves averaged over the three experiments are shown in Figure 1. It can be seen from Figure 1 that the yield of carbon nanotubes and the initial rate of their growth increase with increasing synthesis temperature. Each curve shows a tendency to attenuate the process. Each curve has an induction period - the time of formation of active catalyst centers. With an increase in temperature, the induction period decreases, i.e. the active centers of the catalyst are formed more rapidly.

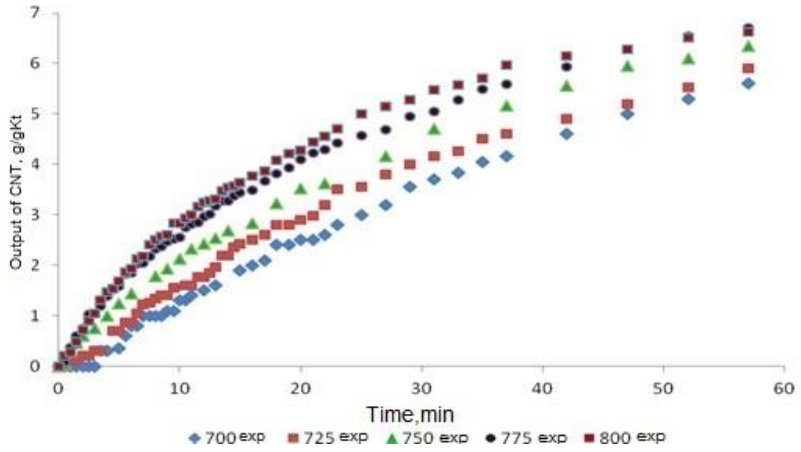

Figure 1: Kinetic curves for the synthesis of carbon nanotubes on the catalyst [Fe0,45Co0,15Al0,40] 2O3 at various temperatures

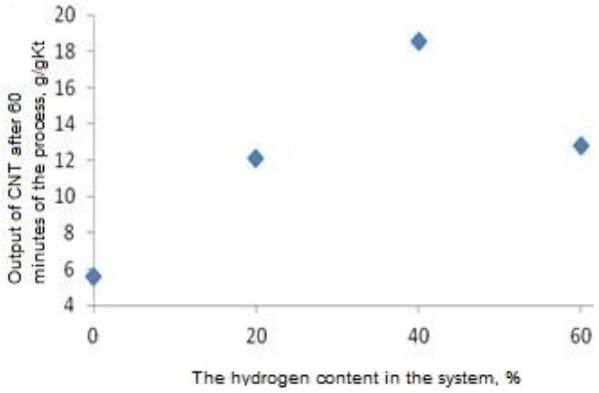

Figure 2: Dependence of the product yield after 60 minutes of the process from the hydrogen content in the feed gas mixture

In the third series of experiments, the initial gas, methane, was diluted with hydrogen. The hydrogen content in the mixture was 5, 20, 40 and 60 % by volume, the catalyst was $[Fe_{0.45}Co_{0.15}Al_{0.40}]_2O_3$, the temperature was 700 ° C. Figure 2 shows the dependence of the yield of carbon nanotubes after 60 minutes of the experiment on the hydrogen content in the mixture. The dependence is extreme, with the highest yield of the product at 40% hydrogen content in the mixture (18.5 g/gKt, which is almost 3 times greater than in pyrolysis of pure methane). Thus, based on experimental studies, optimal conditions were found for obtaining CNT (catalyst composition, synthesis temperature, hydrogen content in the mixture).

2.2 Experimental research in the field of nanocomposite production

The problem of the experiment consisted in the synthesis of a composite material based on Al_2O_3 - ZrO_2 - Y_2O_3 and carbon nanotubes. The content of carbon nanotubes was 0.5 and 1 % by volume. CNT were used which were subjected to mild and severe oxidation. As a result, a composite with an equicrystalline structure and a uniform distribution of nanotubes in the matrix was obtained.

The following types of tubes were used in the work:

CNT-Hard-carbon nanotubes modified by treatment in a mixture of sulfuric and nitric (1: 1) acids (6 h of heat treatment at 110 ° C) - "hard" oxidation;

CNT-Soft - carbon nanotubes modified by treatment in a mixture of sulfuric and nitric (8: 5) acids (heat treatment at 60 ° C for 2 h) - "soft" oxidation.

According to the literature data (Polyakova et al., 2016) under processing under mild conditions, the surface of the CNT is insignificantly hydroxylated. Oxidation under severe conditions leads to a significant degree of surface functionalization, not only hydroxyl, but also carboxyl and ketone groups are present. The introduction of functional groups occurs not only on the outer surface of the CNT, but also on the inner surface, that is, on the walls of the pores.

The preparation process consisted of the following stages:

- Using the method of reverse heterophase deposition and heat treatment, the preparation of the Al_2O_3 - ZrO_2 - Y_2O_3 composite, which has a triple eutectic in the ratio of 52.3% - 39.44% - 8.25%;
- The dispersion of CNTs was carried out by ultrasonic action in an aqueous solution of polyvinyl alcohol (1%);
- Homogenization of the Al_2O_3 - ZrO_2 - Y_2O_3 - CNT suspension using a planetary mill;
- Composite powder drying;
- Spark plasma sintering at a residual pressure of 20 kN and various temperature regimes and with different holding times (Table 2).

The choice of the sintering method is determined by the need to obtain a material with improved mechanical characteristics. A temperature sintering regime was chosen that provided the necessary porosity and preservation of the internal structure of the material (preservation of the crystal size of the matrix, preservation of CNTs). The short duration of the spark plasma sintering process (5-10 minutes) makes it possible to limit the recrystallization of the matrix grain and, using the optimum sintering regime, obtain low-porosity composite materials.

Table 2 shows the properties of composites. A sample containing 0.5 % of hard CNTs has a bending strength of 872 MPa, with a 1 % hard bending strength of 612 MPa. Composite containing 1 % of soft CNTs shows the best result up to 1,030 MPa. Such properties are due to the difference in specific surfaces during the oxidation of CNTs, in hard CNTs of 17.15 m^2/g, in soft to 234. All samples have microhardness necessary for their use.

Table 2: Sintering modes of samples

Type and content of CNTs, %	Sintering temperature, °C	Holding time, min	Heating time, min	Density, g/cm^3	Bending strength, MPa	Average microhardness, GPa
0.5 % hard	1,650	5	3	4.6	872	16.8
1 % hard	1,600	10	3	4.78	612	17.1
1 % soft	1,600	7	3	4.692	998-1,031	17.7

3. Mathematical modeling of CNT synthesis

The gas phase contains two components: methane, hydrogen. The mathematical model has the form:

$$\frac{\partial C_i}{\partial t} + v_1 \frac{\partial C_i}{\partial x} = D_i \frac{\partial^2 C_i}{\partial x^2} + D_i \frac{\partial^2 C_i}{\partial r^2} + \frac{D_i}{r} \frac{\partial C_i}{\partial r} \quad (1)$$

Initial condition:

$$C_i(t=0,x,r)=0 \tag{2}$$

The boundary conditions for Eq(1) should take into account the supply of the initial gas mixture to the reactor, as well as the change in the concentration of the components as a result of the reactions taking place on the catalyst:

$$\begin{cases} C_i(x=0,r)=C_i^{in}(r) \\ \left.\dfrac{\partial C_i}{\partial x}\right|_{x=l}=0 \end{cases} \tag{3}$$

$$\begin{cases} \left.D_i\dfrac{\partial C_i}{\partial r}\right|_{r=0}=\begin{cases}\sum\limits_{j=1}^{m_2}\nu_j^i\bar{W}_j, & x=l_{ap}/2\\ 0, & x\neq l_{ap}/2\end{cases} \\ \left.D_i\dfrac{\partial C_i}{\partial r}\right|_{r=D_{ap}/2}=0 \end{cases} \tag{4}$$

Where t - time, s; C_i - the concentration of the i-th component of the gas phase, mol / m^3; v_1 is the linear velocity of the gas mixture, m / s; D_i - the diffusion coefficient of the i-th component of the gas phase, m^2 / s; x and r - the longitudinal and transverse coordinates of the reactor, m (the origin of the x-axis is the entry point of the feed gas mixture into the reactor, along the r-axis is the reactor axis); C_i^{in}- initial concentration of the i-th gas component at the reactor inlet, mol / m^3; l_{ap} and D_{ap} - length and diameter of the apparatus, respectively, m; $\sum_{j=1}^{m_2}\nu_j^i\bar{W}_j$ - the sum of the rates of formation and consumption of the i-th component of the gas phase from reactions occurring on the surface of the catalyst, mol / (m^3 • s); W_j- velocity of the j-th surface reaction, mol / (m^3 • s); v_i^j - stoichiometric coefficient of the i-th component of the gas phase in the j-th surface reaction. Table 3 presents the kinetic scheme and the values of the kinetic constants obtained from the comparison of the calculated (from the model (1) - (4)) and experimental data.

Table 3: Kinetic scheme of pyrolysis of methane and methane-hydrogen mixtures

№ of stage	The reactions on the catalyst	Stage speed $\tilde{W}_i$	$\tilde{k}_j^0$	$\tilde{E}_j$,kJ/mole
1	Kt + CH_4 → [CH_3-Kt] + H	$\tilde{W}_1=\tilde{k}_1\tilde{C}_{Kt}\bar{C}_{CH_4}$	$4.37\cdot10^{-5}$	91.12
2	[CH_3-Kt] + H → [CH_2-Kt] + H_2	$\tilde{W}_2=\tilde{k}_2\tilde{C}_{[CH_3-Kt]}\bar{C}_H$	$1.10\cdot10^{6}$	71.83
3	[CH_2-Kt] + H → [CH-Kt] + H_2	$\tilde{W}_3=\tilde{k}_3\tilde{C}_{[CH_2-Kt]}\bar{C}_H$	$1.10\cdot10^{6}$	71.83
4	[CH-Kt] + H → [C-Kt] + H_2	$\tilde{W}_4=\tilde{k}_4\tilde{C}_{[CH-Kt]}\bar{C}_H$	$1.10\cdot10^{6}$	71.83
5	[C-Kt] → C_{HT} + Kt	$\tilde{W}_5=\tilde{k}_5\tilde{C}_{[C-Kt]}$	$3.67\cdot10^{5}$	2
6	[C-Kt] → [C_A-Kt]	$\tilde{W}_6=\tilde{k}_6\tilde{C}_{[C-Kt]}$	$5.6\cdot10^{6}$	13.18
7	[C_A-Kt] + 4H → Kt + CH_4	$\tilde{W}_7=\tilde{k}_7\tilde{C}_{[CA-Kt]}\bar{C}_H$	8.07	3.10
8	Kt + H_2 → [H-Kt] + H	$\tilde{W}_8=\tilde{k}_8\tilde{C}_{Kt}\bar{C}_{H_2}$	0.02	46.68
9	[H-Kt] + H → Kt + H_2	$\tilde{W}_9=\tilde{k}_9\tilde{C}_{[H-Kt]}\bar{C}_H$	16.21	48.57

The kinetic scheme of pyrolysis of methane-hydrogen mixtures contains 9 stages, allowed to simulate and explain the character of the kinetic curves of CNT synthesis. Using a mathematical model, it is established that the maximum yield of CNTs can be achieved with a 34 % hydrogen content in the original methane-hydrogen mixture.

4. Mathematical modeling of the process of spark plasma sintering

The fact that the physical and mechanical properties of composites depend on the porosity of the material makes it possible to use this characteristic as the basis for constructing a mathematical model. In compiling a mathematical description of the change in the porosity of the powder body during spark plasma sintering, the physico-chemical essence of the proceeding processes was accounted for by including the following parameters in the model: the heating rate, the maximum heating temperature, the holding time at the maximum temperature,

the CNT content in the composite, the current state of the powder compact current temperature, current pore size).

To describe the process of decreasing the porosity in the sintering process, we introduce the pore size distribution function f (t, l), where t is the time, l is the pore diameter. This function reflects the state of the powder compact at time t. The basic equation describing the process of reducing the pore size (Fedosova et al., 2016):

$$\frac{\partial f}{\partial t} - \frac{\partial f \eta(t,l)}{\partial l} = 0; \; t \in [0;T]; \; l \in [0;L], \tag{5}$$

f(t, l) - the pore size distribution function, t - the process time, η - the pore penetration rate, and l - the pore diameter.

For the first sintering step (heating stage), the driving force of the pore reduction process is the heating rate $\frac{\Delta T}{\Delta t}$, where l - the current pore diameter, T - the current temperature, and V_{CNT} - the volume fraction of the CNT. For the second stage, the driving force is the difference T_{max} - the sintering temperature and $T_{\Delta l}$ - the shrinkage rate change temperature. The following relations are introduced:

$$\eta_1 = k_1 \left(\frac{\Delta T}{\Delta t} \right)^{m_1}, \qquad \begin{cases} k_1 = a_1 + b_1 \sqrt{l^3} + c_1 T \\ a_1 = a_{10} + b_{10} V_{CNT} + c_{10} V_{CNT}^2 \end{cases} \tag{6}$$

$$\eta_2 = k_2 \left(T_{\max} - T_{\Delta l} \right)^{m_2}, \qquad \begin{cases} k_2 = a_2 + b_2 \sqrt{l^3} \\ a_2 = a_{20} + b_{20} V_{CNT} + c_{20} V_{CNT}^2 \end{cases} \tag{7}$$

η_1 and η_2 - the rate of decrease in the pore size at the 1st and 2nd stage of sintering; k1 and k2 - the phenomenological coefficients taking into account the dependence of the pore reduction rate on the number of CNTs, V_{CNT} (parameters a1 and a2), the current pore size l, and the current temperature of the furnace chamber T; m1 and m2 - constants characterizing the degree of deviation of the system from equilibrium for the 1 st and 2 nd stages of sintering, respectively.

To solve Eq(5), we used the absolutely stable scheme of difference approximation developed by us, the "Z-scheme" (the scheme has a second order of approximation with respect to time t and coordinate) (Fedosova et al., 2016).

The difference scheme looks like:

$$\frac{f_j^{n+1} - f_j^n}{\Delta t} - \frac{1}{2} \left(\frac{f_{j+1}^{n+1} \eta_{j+1}^{n+1} - f_j^{n+1} \eta_j^{n+1}}{\Delta l} + \frac{f_j^n \eta_j^n - f_{j-1}^n \eta_{j-1}^n}{\Delta l} \right) = 0 \tag{8}$$

Δt - the time step, Δl - the coordinate step (pore size), the index n - the time step, and the index j - the step along the coordinate.

We assume that the pores in the initial compact of the composite powder are evenly distributed throughout the volume, and their size distribution obeys the law of normal distribution. We give the initial condition for Eq(6) according to this assumption:

$$f(t=0,l) = f^0(l) = \frac{1}{\sigma\sqrt{2\pi}} e^{\frac{(1-\mu)^2}{2\sigma^2}} \tag{9}$$

σ - the standard deviation of the distribution, μ is the average pore diameter, and l is the pore diameter.

The right boundary condition corresponds to the absence of pores of maximum diameter (L_{max}):

$$f(t, l = L_{\max}) = 0 \tag{10}$$

The value of the porosity was calculated according to the formulas:

$$V_{пор} = \int_0^{L_{\max}} \frac{4\pi}{3} \left(\frac{l}{2} \right)^3 f(l) dl \tag{11}$$

$$\varepsilon = \frac{V_{пор}}{V_{пор} + V_{тв}} 100\% \tag{12}$$

The obtained mathematical model is used for carrying out numerical experiments. By spark plasma sintering to determine the change in the pore size distribution function, the change in the average pore diameter, and the total porosity of the powder compact at each time point.
From the comparison of calculated and experimental data, the kinetic parameters of the mathematical model of sintering were determined. On the basis of the computational experiment, the optimum sintering regime was determined.

5. Conclusions

A mathematical model of CNT synthesis was developed by catalytic pyrolysis of a methane-hydrogen mixture. On the basis of experimental studies and mathematical modeling, optimal conditions for the synthesis of CNTs (temperature -775 ° C, hydrogen content in the mixture -34 %) were determined.
An alumina composite of Al_2O_3 - ZrO_2 - Y_2O_3 was made and investigated with a eutectic composition reinforced with carbon nanotubes.
A mathematical model for the description of the process of spark plasma sintering is developed, which is based on the equation of porosity variation of pressing of composite powder Al_2O_3 - ZrO_2 - Y_2O_3 - CNT. The model reflects the change in the pore size distribution function of a powder compact in size in time.
An analysis of the dependence of the rate of decrease in the pore on the first and second stages of spark plasma sintering is given. It is revealed that for heating stage of the powder of the Al_2O_3 - ZrO_2 - Y_2O_3 - CNT composite, the driving force of the porosity reduction process is the heating rate. It is determined that for the second stage the driving force of the porosity reduction process is the difference between the soaking temperature and the temperature of the shrinkage speed variation of the Al_2O_3 - ZrO_2 - Y_2O_3 - CNT composite.
Optimal modes of sintering (heating rate, temperature and holding time) are determined on the basis of experimental studies and mathematical modeling for the Al_2O_3 - ZrO_2 - Y_2O_3 - CNT composite, which ensure high bending strength (870-1,031 MPa) at zero porosity.

Acknowledgments

The work was supported by the Ministry of Education and Science of the Russian Federation under the Grant Agreement No. 14.583.21.0064, the unique identifier of the work (project) RFMEFI58317X0064.

Reference

Bogdanovskaya V.A., Zhutaeva G.V., Radina M.V., Kazansky L.P., Tarasevich M.R., Skichko E.A., Gavrilova N.N., Koltsova E.M., 2016. Physico-chemical properties of carbon nanotubes as carriers for cathode catalysts of fuel cells. Surface Structure and Corrosion Resistance, Physicochemistry of the Surface and Protection of Materials, 52(1), 41-51.

Fedosova N.A., Faikov P.P., Popova N.A., Koltsova E.M., Zharikov E.V., 2015. Ceramic Composite Material Obtained by Spark Plasma Sintering Technology with Carbon Nanotubes. Glass and Ceramics, 1(72), 13-16.

Fedosova N.A., Koltsova E.M., Zharikov E.V., Mitrichev I.I., Shaneva A.S., 2016. Spark plasma sintering simulation of alumina composite modified with carbon nanotubes, Chemical Engineering Transactions, 52, 979-984.

Polyakova Y.A., Myachina M.A., Gavrilova N.N., 2016. Functionalization of carbon nanotubes for creation of the dispersed system ZrO2-CNT, Success in Chemistry and Chemical Technology, XXX(1), 87-89.

Skichko E.A., Lomakin D.A, Gavrilov Yu.V., Koltsova E.M.,2012. Experimental investigation of the kinetic regularities of the synthesis of carbon nanotubes of catalytic pyrolysis of gas mixtures of variable composition, Fundamental Research, 3 (2), 414-418.

Suárez M., Fernández A., Menéndez J.L., Torrecillas R., Kessel H.U., Hennicke J., Kirchner R., Kessel, T., 2013. Challenges and opportunities for spark plasma sintering: a key technology for a new generation of materials, INTECH Open Access Publisher, 15, 58-60.